SIMULATION OF RUNAWAY ELECTRON AVALANCHE IN ITER DISRUPTION

[1]Z.K. Yu, F. Wang, X.F. Wu and Z.X. Wang, [2]S.J. Liu, [3]D. Hu

[1]School of Physics, Dalian University of Technology, Dalian, China
[2]Max Planck Institute for Plasma Physics, Garching, Germany
[3]School of Physics, Beihang University, Beijing 100191, People's Republic of China
Email: fengwang@dlut.edu.cn

1. RUNAWAY ELECTRON AVALANCHE MODEL

The avalanche of runaway electrons, triggered by large-angle collision of traces of seed electrons with the bulk electron population, presents a critical challenge for tokamak operations in devices like ITER. Through integrated simulations combining the PTC code [1] and JOREK MHD code [2,3], we investigate the nonlinear dynamics of runaway electron avalanches during ITER disruption events, with particular emphasis on (i) the exponential growth phase and (ii) the critical threshold for avalanche initiation. The numerical framework incorporates a guiding-centre formulation with three key components: (i) small-angle collision operator for Coulomb scattering, (ii) large-angle collision operator based on Møller differential cross-sections, and (iii) synchrotron radiation losses. These components are evaluated under disruption scenarios characterized by n = 0 toroidal mode number electromagnetic field configurations. Seed electrons originate from the high-energy tail of the pre-thermal-quench electron population, described by a relativistic Maxwell-Jüttner distribution.

2. SIMULATION RESULTS

The temporal evolution of the runaway electron population at three time slices are shown in figure 1. It is found that the runaway electron avalanche is observed only at the phase of the thermal quench, when the electric field accelerate the transformation from secondary electrons to seed electrons, providing the particle source of large-angle collision.

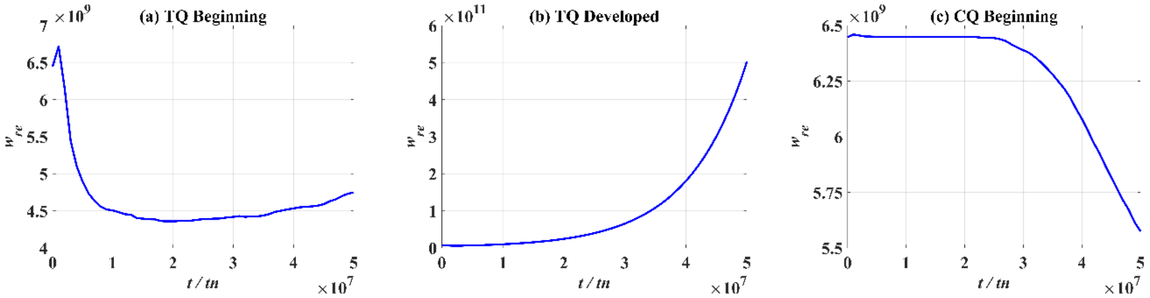

FIG. 1. The number of runaway electrons as a function of time normalized to the cyclotron period tn = 5.69×10^{-12} (s) at the three time slices: (a) the beginning of the thermal quench; (b) the phase of the thermal quench; (c) the beginning of the current quench. The initial energy of the particles is taken to be the same $\gamma = 3.16$, with an isotropic pitch-angle distribution.

The absence of runaway avalanche in the other disruption phases can be attributed to the following factors: (1) The runaway formation by avalanche is largely compensated for by lost particles decelerated by the complex local electric field and small-angle collision to below the critical energy for electron runaway chosen to be $\gamma = 2.0$. This effect is evident at the beginning of the thermal quench. (2) the weak local electric field lacks the strength to accelerate secondary electrons the critical energy for large-angle collision chosen to be $\gamma = 3.0$, limiting the generation of new runaway electrons. Furthermore, the pitch angle scattering effect and the trapping effect induced by the toroidicity also play an essential role in the runaway electron avalanche. The momentum-space distributions of runaway electrons are shown in figure 2. The momentum of runaway electrons becomes significant anisotropic at the beginning of the thermal quench and the phase of the thermal quench, while remaining isotropic at the beginning of the current quench. The result reveals that the parallel electric field reaches its maximum strength and is nearly anti-aligned with the magnetic field at the phase of the thermal quench, sufficient to overcome the deflecion by pitch-angle scattering and lead to an anisotropic of electron momentum. It is also found that a portion of runaway electrons are trapped around $p_{||} = 0$ at the beginning of the thermal quench and current quench. They are predominantly composed of secondary electrons generated by large-angle scattering, and trapped for a long duration due to the positive and negative gradients of the parallel electric field. These analyses provide insights into the avalanche of runaway electrons in disruption scenarios.

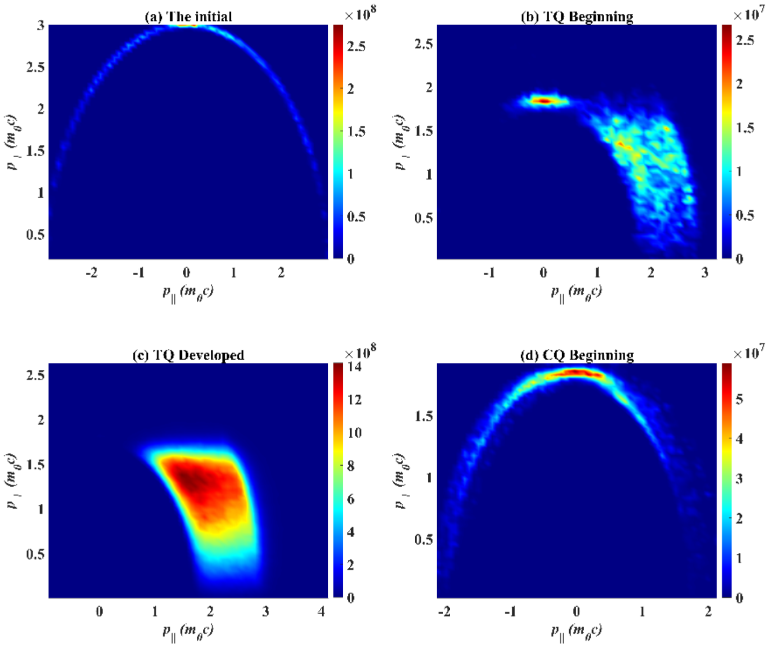

FIG. 2. The initial (a) and final (b)(c)(d) momentum-space distributions of runaway electrons at the three time slices: (b) the beginning of the thermal quench; (c) the phase of the thermal quench; (d) the beginning of the current quench.

ACKNOWLEDGEMENTS

This work has been financially supported by the National Key R&D Program of China (Grant No. 2022YFE03090000), the National Natural Science Foundation of China (Grant No. 12435014) and the Fundament Research Funds for the Central Universities (Grant Nos. DUT24GF110 and DUT24ZD403).

REFERENCES

[1] Wang F., Zhao R., Wang Z.X., Zhang Y., Lin Z.H., Liu S.J. and CFETR Team., PTC: Full and drift particle orbit tracing code for α particles in tokamak plasmas, CHIN. PHYS. LETT. **38** 5 (2021) 055201.

[2] Hu D., Nardon. E., Artola F.J., Lehnen M., Bonfiglio D., Hoelzl M., Huijsmans G.T.A., Lee S.-J., and the JOREK Team., Collisional-radiative simulation of impurity assimilation, radiative collapse and MHD dynamics after ITER shattered pellet injection, Nucl. Fusion **63** 6 (2023) 066008.

[3] Hoelzl M. et al., The JOREK non-linear extened MHD code and applications to large-scale instabilities and their control in magnetically confined fusion plasmas, Nucl. Fusion **61** 6 (2021) 065001.